

# The Araucaria Project. The Distance to the Small Magellanic Cloud from Near-Infrared Photometry of RR Lyrae Variables <sup>1</sup>

Olaf Szewczyk

*Universidad de Concepción, Departamento de Astronomía, Casilla 160-C, Concepción,  
Chile*

szewczyk@astro-udec.cl

Grzegorz Pietrzyński

*Universidad de Concepción, Departamento de Astronomía, Casilla 160-C, Concepción,  
Chile*

*Warsaw University Observatory, Al. Ujazdowskie 4, 00-478, Warsaw, Poland*

pietrzyn@astrouw.edu.pl

Wolfgang Gieren

*Universidad de Concepción, Departamento de Astronomía, Casilla 160-C, Concepción,  
Chile*

wgieren@astro-udec.cl

Anna Ciechanowska

*Warsaw University Observatory, Al. Ujazdowskie 4, 00-478, Warsaw, Poland*

aciechan@astrouw.edu.pl

Fabio Bresolin

*Institute for Astronomy, University of Hawaii at Manoa, 2680 Woodlawn Drive, Honolulu  
HI 96822, USA*

bresolin@ifa.hawaii.edu

Rolf-Peter Kudritzki

*Institute for Astronomy, University of Hawaii at Manoa, 2680 Woodlawn Drive, Honolulu  
HI 96822, USA*

kud@ifa.hawaii.edu

## ABSTRACT

We have obtained deep infrared  $J$  and  $K$  band observations of nine  $4.9 \times 4.9$  arcmin fields in the Small Magellanic Cloud (SMC) with the ESO New Technology Telescope equipped with the SOFI infrared camera. In these fields, 34 RR Lyrae stars catalogued by the OGLE collaboration were identified. Using different theoretical and empirical calibrations of the infrared period-luminosity-metallicity relation, we find consistent SMC distance moduli, and find a best true distance modulus to the SMC of  $18.97 \pm 0.03$  (statistical)  $\pm 0.12$  (systematic) mag which agrees well with most independent distance determinations to this galaxy, and puts the SMC 0.39 mag more distant than the LMC for which our group has recently derived, from the same technique, a distance of 18.58 mag.

*Subject headings:* distance scale - galaxies: distances and redshifts - galaxies: individual(SMC) - stars: RR Lyrae - infrared: stars

## 1. Introduction

In our ongoing Araucaria Project (e.g. Gieren et al. 2005a), we are applying a number of different stellar standard candles to independently determine the distances to a sample of nearby galaxies. The systematic differences between the distance results obtained for the individual galaxies from the various stellar candles will be analyzed in forthcoming papers. This analysis is expected to lead to a detailed understanding of how the various stellar techniques, which are fundamental to calibrate the first rungs of the distance ladder, depend on metallicity and age. While the objects we use for the distance determinations are usually detected from optical wide-field imaging surveys of the target galaxies (e.g. Pietrzyński et al. 2002b), the most accurate distance work is then done from follow-up near-infrared images which virtually eliminate reddening as a significant source of error on the results. Examples of this very successful approach are the Cepheid work on the Sculptor galaxies NGC 300 (Gieren et al. 2005b), NGC 55 (Gieren et al. 2008) and NGC 247 (Gieren et al. 2009), and the red clump star work on the LMC (Pietrzyński & Gieren 2002). The Araucaria Project has also been developing a new spectroscopic distance indicator, viz. the Flux-weighted Gravity- Luminosity Relationship (FGLR) for blue supergiants (Kudritzki et al. 2003; 2008)

---

<sup>1</sup>Based on observations obtained with the ESO NTT for programmes 082.D-0513(A) and 079.D-0482(A)

which is able to yield distances accurate to 5% to galaxies containing massive blue stars out to about 10 Mpc from low-resolution spectra (Kudritzki et al. 2008, Urbaneja et al. 2008).

Thanks to several recent theoretical and empirical studies, evidence has been mounting that RR Lyrae (RRL) stars are excellent standard candles in the near-infrared spectral range, providing distance results which are superior to the traditional optical method (e.g. Bono 2003a). Longmore et al. (1986) were the first to show that RRL variable stars follow a period-luminosity (PL) relation in the near-infrared K-band. Their pioneering work was followed by Liu & Janes (1990), Jones et al. (1996), and Skillen et al. (1993), who applied infrared versions of the Baade-Wesselink method to calibrate the luminosities and distances of RRL stars. A very comprehensive analysis of the IR properties of RRL stars was given by Nemec et al. (1994). The first theoretical constraints on the K-band PL relation of RRL stars are based on non-linear convective pulsation models which were presented by Bono et al. (2001). Dall’Ora et al. (2004) later demonstrated that the K-band PL relation for RRL stars appears to have a very small scatter for globular clusters, with small intrinsic spread in metallicity for this type of stars. Further theoretical explorations of the RRL period-mean magnitude-metallicity relations in near-infrared passbands were carried out by Bono et al. (2003b), Catelan et al. (2004), and Cassisi et al. (2004). Most recently, Sollima et al. (2008) analyzed near-infrared K-band data of RRL stars in some 15 Galactic globular clusters and provided the first empirical calibration of the period-luminosity-metallicity (PLZ) relation in the *K* band. All these existing theoretical and empirical studies have suggested that the RRL star K-band PLZ relation appears to be a superb means to determine accurate distances to galaxies hosting an abundant old stellar population.

We have therefore started to include this tool in the Araucaria Project distance work. In previous papers, we determined the distance to the Sculptor dwarf galaxy (Pietrzyński et al. 2008), and to the LMC (Szewczyk et al. 2008) from this method. In this paper, we apply the technique to a sample of RR Lyrae stars distributed over the SMC, and determine the distance to the SMC for the first time with the infrared RR Lyrae technique.

## 2. Observations, Data Reduction and Calibration

During several observing runs of the Araucaria Project, we have obtained all the data analyzed and presented in this paper with the SOFI infrared camera attached to the ESO New Technology Telescope. The Large Field setup was used to yielding a  $4.9 \times 4.9$  arcmin field of view and a scale of 0.288 arcsec per pixel.

It was possible to collect deep *J*s and *K*s images of six distinct SMC fields during 3

nights in 2007, and of three more fields over 2 nights in 2008. All but one nights were found to have photometric conditions. Detailed information on each observed field can be found in Table 1. Figure 1 illustrates the location of the observed fields on an image of the SMC. In order to take into account the rapid sky level variations in the IR passbands, we have been using a dithering technique during the observations. Total integration times per field were 60 min in the  $Ks$  band, and 15 min in the  $Js$  band.

For all the reductions and calibrations, the pipeline developed in the course of the Araucaria Project was used. As a first step, the subtraction of sky level subprocess (including the masking of stars with the IRAF xdimsum package) was applied (Pietrzyński & Gieren 2002). Later, each single image was flatfielded and stacked into the final deep field. PSF (point spread-function) photometry with aperture corrections was then performed in the same way as described in Pietrzyński et al. (2002b).

The photometry was calibrated onto the standard system using observations of 15 standard stars from the UKIRT list (Hawarden et al. 2001). All of them were observed under photometric conditions at different airmasses spread in between the regular target fields acquisition. The data obtained during the non-photometric night was compared with nearby photometric data and the zero-point difference was estimated. Thanks to the large number of standard stars observed, the accuracy of our photometric zero points was estimated to be as good as 0.02 mag. The results were compared with the Two Micron All Sky Survey (2MASS) catalog for common stars. This way we could determine the zero point differences which are given in Table 2. The calibrated NIR magnitudes for all RRL stars identified in our science target fields are presented in Table 3. All uncertainties given in the Tables are standard deviations.

### 3. Near-Infrared Period-Luminosity Relations

The final sample of 34 RRL stars analyzed in our SOFI/NTT fields was chosen by rejecting all stars which were blended with or contaminated by other close-by objects in the frames. Then it was cross-identified with the Optical Gravitational Lensing Experiment (OGLE) catalog of RRL stars in the SMC (Soszyński et al. 2002). The positions of the RRL stars in the  $K$ ,  $J - K$  color-magnitude diagram are shown in Figure 2. All variables have at least one measurement collected during photometric conditions. In the case of RRL stars which were observed more than once, we took a straight average of the random-phase magnitudes, which is expected to lead to a better approximation of their mean magnitudes.

Following the identification from the OGLE catalog (Soszyński et al. 2002), we fun-

damentalize the RRc periods by adding  $\log(P) = 0.127$  in order to combine the RRab and RRc stars. We have corrected the observed magnitudes for extinction, adopting the reddening values published by Udalski et al. (1999) which are shown in Table 1. Adopting the reddening law from Schlegel et al (1998), we calculate the following selective extinctions in the different bands:  $A_K = 0.367E(B - V)$  and  $A_J = 0.902E(B - V)$ . The final photometric data for the sample of RRL stars are presented in Table 4. The PL relations for the  $J$  and  $K$  bands derived from our magnitudes are shown in Figure 3.

The relatively large scatter seen in Figures 2 and 3 are mainly caused by four factors: (1) the random single-phase nature of our IR measurements, which represents the mean magnitude of an RRL variable only to  $\sim 0.15$  mag (e.g. Del Principe et al. 2006), (2) the metallicity spread among the RRL stars in SMC, (3) the depth extension of the SMC in the line of sight, and (4) the accuracy of our single measurements which is  $0.03 - 0.11$  mag for stars of magnitudes of  $18.0 - 19.0$  mag in the  $K$ -band.

We compare the PL relations derived from the observed RRL stars against the existing theoretical (Bono et al. 2003; Catelan et al. 2004) and empirical (Sollima et al. 2008) relations. Table 5 lists our results for the slope and zero-point values of the PL relations and as well as those from the theoretical and empirical ones.

#### 4. The Distance Determination

In order to derive the apparent distance moduli to the SMC from our data, we used the following calibrations of the NIR PL relations of mixed population RRL stars:

$$M_K = -1.07 - 2.38 \log P + 0.08[Fe/H] \quad - \text{ Sollima et al. (2008)} \quad (1)$$

$$M_K = -0.77 - 2.101 \log P + 0.231[Fe/H] \quad - \text{ Bono et al. (2003b)} \quad (2)$$

$$M_K = -0.597 - 2.353 \log P + 0.175 \log Z \quad - \text{ Catelan et al. (2004)} \quad (3)$$

$$M_J = -0.141 - 1.773 \log P + 0.190 \log Z \quad - \text{ Catelan et al. (2004)} \quad (4)$$

We recall that the calibration of Sollima et al. (2008) was constructed for the 2MASS photometric system, while the calibrations of Catelan et al. (2004) and Bono et al. (2003)

are usable for the Glass or Bessel & Brett systems, respectively. Therefore we transformed our own data, calibrated onto the UKIRT system (Hawarden et al. 2001), to the Glass and Bessel & Brett systems using the transformations presented by Carpenter (2001) before calculating distances using the calibrations of Catelan et al. (2004) and Bono et al. (2003). Since there is no significant difference between the  $K$ -band of 2MASS and UKIRT systems (Carpenter 2001), we did not apply any transformations to our data while using the Sollima et al. (2008) calibration.

Assuming the mean metallicity of RRL stars in the SMC to be  $[Fe/H] = -1.7$  dex (e.g. Udalski 2000) we have calculated the  $K$ - and  $J$ -band distance moduli for our sample of RRL stars using the final photometric magnitudes as given in Table 4. The fits for the relations (1) – (4) to both sets of data are displayed in Figure 4.

The true distance moduli of the SMC obtained from the different PLZ calibrations are summarized in Table 6. As our best distance determination, we adopt the average value from the different calibrations, yielding 18.97 mag. The uncertainty on this value will be discussed in the next section.

## 5. Discussion

The distance moduli obtained from several independent theoretical and empirical calibrations of the infrared RR Lyrae PLZ relation are consistent. The maximum difference of 0.06 mag between the results from the calibrations of Sollima et al. (2008) and Bono et al. (2003b) is certainly not significant taking into account all the uncertainties, which affect the whole process of constructing these calibrations. It is interesting to note that a very similar difference between the distance moduli derived using these two calibrations was recently obtained by Pietrzyński et al. (2008) for the Sculptor galaxy ( $[Fe/H] = -1.83$  dex). Therefore, perhaps there is just a zero point offset in the sense that the distances from the calibration of Sollima et al. (2008) are slightly shorter compared to those from the calibration of Bono et al. (2003b).

Taking into account the errors associated with the adopted calibrations, mean metallicity, photometric zero point and absorption correction, we estimate the systematic error of our distance determination to be of 0.12 mag. Therefore our best distance modulus determination to the SMC is:  $18.97 \pm 0.03$  (statistical)  $\pm 0.12$  (systematic) mag. This value agrees very well with the value of  $18.967 \pm 0.018$  mag derived from  $K$ -band photometry of red clump stars (Pietrzyński, Gieren & Udalski 2003). It also agrees, within the combined  $1\sigma$  uncertainties, with the true SMC distance modulus derived from Cepheid variables (e.g.

Udalski 2000; Barnes et al. 1993). The distance modulus of the SMC found in this paper is 0.39 mag larger than the value for the LMC we found from the same technique (Szewczyk et al. 2008). Again, this difference is very much in line with modern values found from other techniques, like Cepheid variables (0.5 mag; Udalski 2000), and red clump stars (0.47 mag; Pietrzyński, Gieren & Udalski 2003).

We do not observe any significant difference in the dispersions of the NIR P-L relations defined by the RR Lyrae variables in the SMC (this paper), and the LMC (Szewczyk et al. 2008), arguing against a more significant distance spread in the line of sight in the SMC than in the LMC, as usually found for younger tracers like Cepheids.

## 6. Summary and Conclusions

The results of our deep infrared imaging and photometry of 34 RR Lyrae stars spread over nine  $4.9 \times 4.9$  arcmin fields in the SMC are presented. Our data show two clear sequences in the period luminosity plane, which correspond to the RRC and RRab stars. After fundamentalizing the RRC periods to the period of the RRab stars by adding  $\log P = 0.127$ , both groups were merged, and the distance moduli to the SMC were determined using different theoretical and empirical calibrations. Our final adopted distance agrees very well with modern results obtained from a number of different techniques.

Our results confirm that the RR Lyrae period-luminosity-metallicity relations in the near-infrared passbands are potentially a very good tool for accurate distance measurements. In future programs, particularly for the LMC, we want to reduce the systematic uncertainty of our distance determinations with this method by providing multi-phase JK observations of the RR Lyrae variables to determine their mean magnitudes with better precision.

WG and GP gratefully acknowledge financial support for this work from the Chilean Center for Astrophysics FONDAF 15010003, and from the BASAL Center for Astrophysics and Related Technologies (CATA 2007 PFB 06). Support from the Polish grant N203 002 31/046 and the FOCUS subsidy of the Foundation for Polish Science (FNP) is also acknowledged. It is a special pleasure to thank the support astronomers at ESO-La Silla for their expert help in the observations, and the ESO OPC for the generous amounts of observing time at the NTT allocated to our programme.

## REFERENCES

- Barnes, T.G., Moffett, T.J. & Gieren, W., 1993, *ApJ*, 405, L51
- Bono, G., Caputo, F., Castellani, V., Marconi, M. & Storm, J., 2001, *MNRAS*, 326, 1183
- Bono, G., 2003a, in *Stellar Candles for the Extragalactic Distance Scale*, eds. D. Alloin and W. Gieren, *Lecture Notes in Physics*, Vol. 635, p. 85
- Bono, G., Caputo, F., Castellani, V., Marconi, M., Storm, J. & Degl’Innocenti, S., 2003b, *MNRAS*, 344, 1097
- Carpenter, J.M., 2001, *AJ*, 121, 2851
- Cassisi, S., Castellani, M., Caputo, F. & Castellani, V., 2004, *A&A*, 426, 641
- Catelan, M., Pritzl, B.J. & Smith, H.A., 2004, *ApJS*, 154, 633
- Dall’Ora, M., Storm, J., Bono, G., et al., 2004, *ApJ*, 610, 269
- Del Principe, M., Piersimoni, A.M., Storm, J., et al., 2006, *ApJ*, 652, 362
- Gieren, W., Pietrzyński, G., Bresolin, F., et al., 2005a, *Messenger*, 121, 23
- Gieren, W., Pietrzyński, G., Soszyński, I., Bresolin, F., Kudritzki, R.-P., Minniti, D. & Storm, J., 2005b, *ApJ*, 628, 695
- Gieren, W., Pietrzyński, G., Soszyński, I., Bresolin, F., Kudritzki, R.P., Storm, J. & Minniti, D., 2008, *ApJ*, 672, 266
- Gieren, W., Pietrzyński, G., Soszyński, I., Szewczyk, O., Bresolin, F., Kudritzki, R.-P., Urbaneja, M.A., Storm, J. & García-Varela, A., 2009, *ApJ*, 700, 1141
- Hawarden, T.G., Leggett, S.K., Letawsky, M.B., et al., 2001, *MNRAS*, 325, 563
- Jones, R.V., Carney, B.W. & Fulbright, J.P., 1996, *PASP*, 108, 877
- Kudritzki, R.-P., Bresolin, F. & Przybilla, N., 2003, *ApJ*, 582, L83
- Kudritzki, R.-P., Urbaneja, M.A., Bresolin, F., Przybilla, N., Gieren, W. & Pietrzyński, G., 2008, *ApJ*, 681, 269
- Liu, T., and Janes, K.A., 1990, *ApJ*, 354, 273
- Longmore, A.J., Fernley, J.A. & Jameson, R.F., 1986, *MNRAS*, 220, 279
- Nemec, J.M., Nemec, A.F. Linnell & Lutz, T.E., 1994, *AJ*, 108, 222
- Pietrzyński, G., and Gieren, W., 2002, *AJ*, 124, 2633
- Pietrzyński, G., Gieren, W., Fouqué, P. & Pont, F., 2002b, *AJ*, 123, 789
- Pietrzyński, G., Gieren, W., & Udalski, A., 2003, *AJ*, 125, 2494



- Pietrzyński, G., Gieren, W., Szewczyk, O., Rizzi, L., Bresolin, F., Kudritzki, R.-P., Nalewajko, K., Storm, J., Dall’Ora, M. & Ivanov, V., 2008, *AJ*, 135, 1993
- Skillen, I., Fernley, J.A., Stobie, R.S. & Jameson, R.F., 1993, *MNRAS*, 265, 301
- Schlegel, D.J., Finkbeiner, D.P., and Davis, M., 1998, *ApJ*, 500, 525
- Sollima, A., Cacciari, C., Arkharov, A.A., Larionow, V.M., Gorshanov, N.V. & Piersimoni, A., 2008, *MNRAS*, 384, 1583
- Soszyński, I., Udalski, A., Szymański, M., Kubiak, M., Pietrzyński, G., Woźniak, P., Żebruń, K., Szewczyk, O. & Wyrzykowski, Ł, 2002, *Acta Astronomica*, 52, 369
- Szewczyk, O., Pietrzyński, G., Gieren, W., Storm, J., Walker, A., Rizzi, L., Kinemuchi, K., Bresolin, F., Kudritzki, R.-P. & Dall’Ora, M., *AJ*, 136, 272
- Udalski, A., Soszyński, I., Szymański, M., Kubiak, M., Pietrzyński, G. Woźniak, P. & Żebruń, K., 1999, *Acta Astronomica*, 49, 437
- Udalski, A., 2000, *Acta Astronomica*, 50, 279
- Urbaneja, M.A., Kudritzki, R.-P., Bresolin, F., Przybilla, N., Gieren, W. & Pietrzyński, G., 2008, *ApJ*, 684, 118

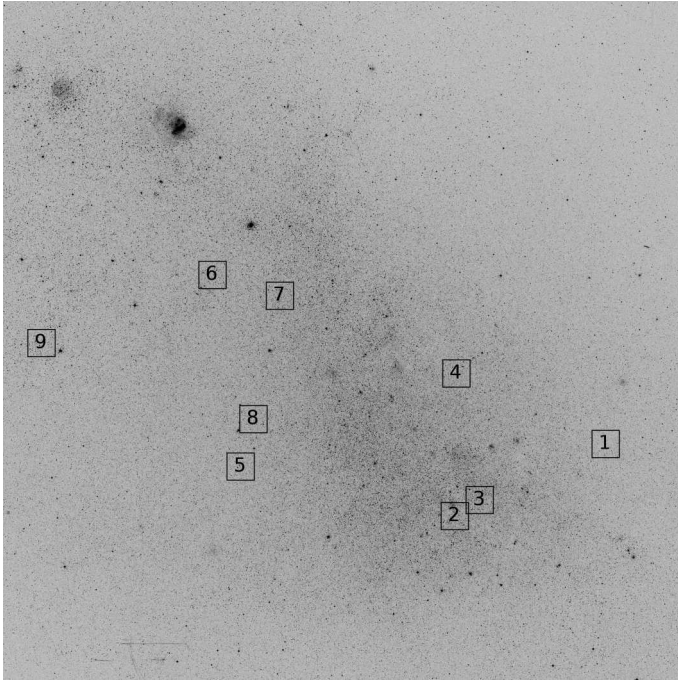


Fig. 1.— The location of our observed  $4.9 \times 4.9$  arcmin NTT/SOFI fields in the SMC on the DSS-1 plate. North is up and east to the left.

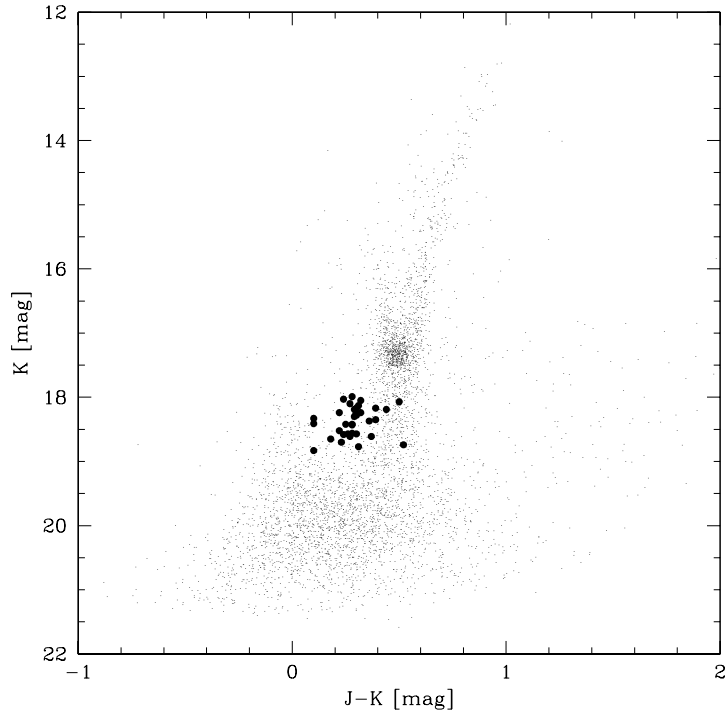


Fig. 2.— The infrared color-magnitude diagram, showing the locations of the RRL stars we have identified in the observed fields.

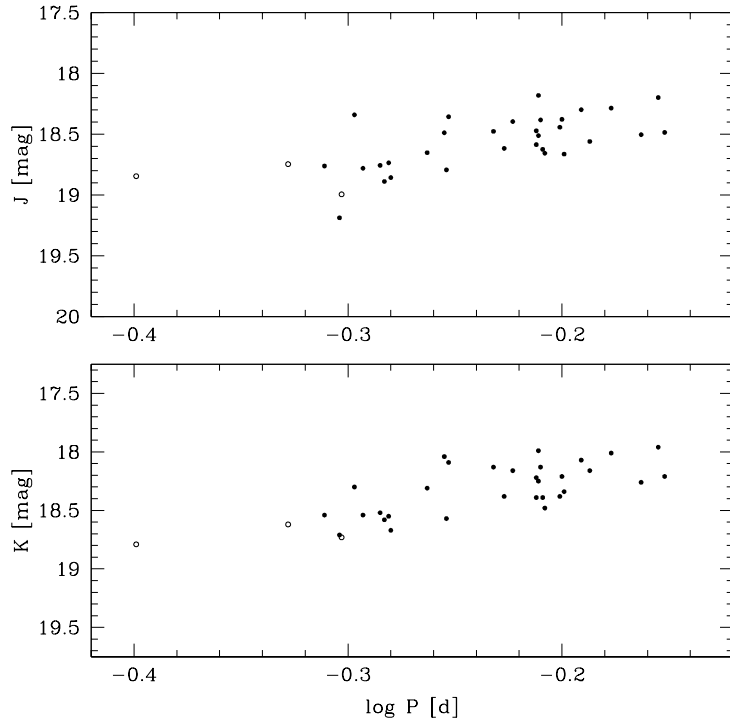


Fig. 3.— The near-infrared  $K$  and  $J$  band period-luminosity relations defined by the RR Lyrae stars observed in the SMC. Period is in days. Fundamental mode pulsators are indicated with filled circles, first overtone pulsators with open circles.

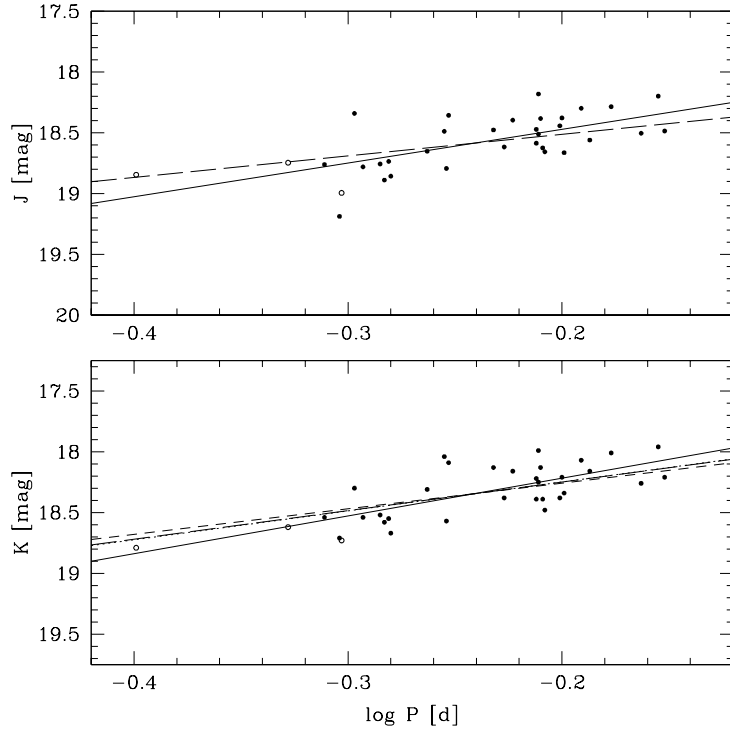


Fig. 4.— The PL relations in  $K$  and  $J$  defined by the RR Lyrae stars observed in the SMC, plotted along with the best fitting lines. The solid, dotted, short- and long-dashed lines correspond to the free fit, and the calibrations of Sollima et al. (2008), Bono et al. (2003b) and Catelan et al. (2004), respectively.

Table 1. Observational information on the target fields. Extinction values are taken from the reddening maps of Udalski et al. (1999).

Field No	Field name	RA2000	DEC2000	Date of observation	MJD of $J_s$ exposure	MJD of $K_s$ exposure	Conditions	Extinction E(B-V)
1	SC2_FI	00:41:57.60	-73:04:30.00	2007-08-27	54340.034307	54340.045077	CLR	0.078
				2007-08-28	54341.170250	54341.178630	STD	
2	SC4_FII	00:47:55.20	-73:18:36.00	2007-08-27	54340.230586	54340.241368	CLR	0.094
				2007-08-28	54341.373742	54341.382950	STD	
3	SC4_FIII	00:46:55.20	-73:15:36.00	2007-08-27	54340.152757	54340.182271	CLR	0.094
				2007-08-28	54341.348700	54341.363482	STD	
4	SC4_FIV	00:48:04.80	-72:53:24.00	2007-08-27	54340.289348	54340.289348	CLR	0.094
				2007-11-24	54429.106746	54429.117547	STD	
5	SC7_FV	00:56:43.20	-73:10:30.00	2007-08-28	54341.195314	54341.206117	STD	0.097
6	SC8_FVI	00:57:50.40	-72:36:36.00	2007-08-28	54341.276830	54341.276830	STD	0.100
7	SC7_FVII	00:55:09.15	-72:40:12.80	2008-12-14	54815.030191	54815.041781	STD	0.097
8	SC7_FVIII	00:56:11.44	-73:02:08.70	2008-12-14	54815.091332	54815.102922	STD	0.097
9	SC10_FIX	01:04:38.40	-72:48:00.00	2008-12-15	54816.038947	54816.050542	STD	0.079

Table 2. Difference of zero point estimation between 2MASS and selected observational data.

Field name	$ 2MASS - J_s $ [mag]	$ 2MASS - K_s $ [mag]
SC7_FV	$0.06 \pm 0.13$	$0.06 \pm 0.08$
SC7_FVIII	$0.07 \pm 0.04$	$0.05 \pm 0.13$

Table 3. Individual  $J_s$  and  $K_s$  Band Observations of RR Lyrae stars in SMC fields

Star ID [OGLE]	Star type	Period [d]	Field name	$J_s$ [mag]	$K_s$ [mag]	Remarks
2008-08-27						
OGLE004211.68-730329.2	ab	0.632047	SC2_FI	$18.724 \pm 0.047$	$18.302 \pm 0.043$	
OGLE004225.29-730349.8	ab	0.699868	SC2_FI	$18.341 \pm 0.039$	$18.088 \pm 0.039$	
OGLE004126.84-730355.2	ab	0.705041	SC2_FI	$18.673 \pm 0.047$	$18.217 \pm 0.043$	
OGLE004154.36-730539.3	ab	0.524564	SC2_FI	$18.850 \pm 0.045$	$18.558 \pm 0.041$	
OGLE004156.46-730641.7	ab	0.586298	SC2_FI	$17.568 \pm 0.027$	$17.111 \pm 0.034$	blend
OGLE004817.88-731815.2	ab	0.558981	SC4_FII	$18.441 \pm 0.039$	$18.232 \pm 0.038$	
OGLE004744.69-731919.1	ab	0.598960	SC4_FII	$18.491 \pm 0.052$	$18.193 \pm 0.038$	
OGLE004805.65-732033.9	ab	0.523798	SC4_FII	$18.748 \pm 0.039$	$18.479 \pm 0.036$	
OGLE004724.96-731427.2	ab	0.614266	SC4_FIII	$18.671 \pm 0.058$	$18.419 \pm 0.040$	
OGLE004649.00-731544.5	ab	0.665961	SC4_FIII	$18.383 \pm 0.041$	$18.126 \pm 0.031$	
OGLE004650.36-731652.2	ab	0.630375	SC4_FIII	$18.495 \pm 0.033$	$18.244 \pm 0.022$	
OGLE004755.07-725141.5	ab	0.504549	SC4_FIV	$18.395 \pm 0.042$	$18.302 \pm 0.034$	
OGLE004805.17-725144.4	ab	0.509540	SC4_FIV	$18.728 \pm 0.054$	$18.515 \pm 0.050$	
OGLE004754.45-725212.1	ab	0.586127	SC4_FIV	$18.475 \pm 0.070$	$18.167 \pm 0.072$	
OGLE004756.26-725217.6	ab	0.592250	SC4_FIV	$18.701 \pm 0.043$	$18.385 \pm 0.037$	
OGLE004800.43-725222.7	ab	0.518919	SC4_FIV	$18.936 \pm 0.047$	$18.553 \pm 0.052$	
OGLE004758.51-725430.6	ab	0.618294	SC4_FIV	$18.614 \pm 0.046$	$18.319 \pm 0.039$	
OGLE004744.89-725530.1	c	0.297777	SC4_FIV	$18.825 \pm 0.057$	$18.855 \pm 0.038$	
OGLE004817.37-725536.5	ab	0.556467	SC4_FIV	$18.690 \pm 0.073$	$18.162 \pm 0.056$	
2008-08-28						
OGLE004211.68-730329.2	ab	0.632047	SC2_FI	$18.742 \pm 0.034$	$18.443 \pm 0.098$	
OGLE004225.29-730349.8	ab	0.699868	SC2_FI	$18.196 \pm 0.030$	$17.898 \pm 0.065$	
OGLE004126.84-730355.2	ab	0.705041	SC2_FI	$18.438 \pm 0.047$	$18.256 \pm 0.088$	
OGLE004154.36-730539.3	ab	0.524564	SC2_FI	$19.004 \pm 0.042$	$18.836 \pm 0.109$	
OGLE004156.46-730641.7	ab	0.586298	SC2_FI	$17.163 \pm 0.036$	$17.260 \pm 0.046$	blend
OGLE004817.88-731815.2	ab	0.558981	SC4_FII	... $\pm$ ...	$18.019 \pm 0.071$	
OGLE004744.69-731919.1	ab	0.598960	SC4_FII	$18.470 \pm 0.035$	$18.192 \pm 0.091$	
OGLE004805.65-732033.9	ab	0.523798	SC4_FII	$18.892 \pm 0.038$	$18.687 \pm 0.110$	
OGLE004724.96-731427.2	ab	0.614266	SC4_FIII	... $\pm$ ...	... $\pm$ ...	
OGLE004649.00-731544.5	ab	0.665961	SC4_FIII	$18.357 \pm 0.034$	$17.969 \pm 0.071$	
OGLE004650.36-731652.2	ab	0.630375	SC4_FIII	$18.430 \pm 0.030$	$18.237 \pm 0.080$	
OGLE005656.87-730850.2	ab	0.545403	SC7_FV	$18.739 \pm 0.063$	$18.346 \pm 0.046$	
OGLE005658.96-730850.6	ab	0.641613	SC7_FV	$18.348 \pm 0.137$	$17.271 \pm 0.030$	contaminated
OGLE005616.96-730901.6	ab	0.615658	SC7_FV	$18.268 \pm 0.032$	$18.030 \pm 0.036$	
OGLE005614.52-731023.8	ab	0.701793	SC7_FV	$16.093 \pm 0.014$	$15.740 \pm 0.011$	blend

Table 3—Continued

Star ID [OGLE]	Star type	Period [d]	Field name	$J_s$ [mag]	$K_s$ [mag]	Remarks
OGLE005612.31-731222.5	ab	0.619898	SC7_FV	$18.743 \pm 0.028$	$18.517 \pm 0.039$	
OGLE005728.85-723454.6	ab	0.416258	SC8_FVI	$19.615 \pm 0.080$	$19.242 \pm 0.101$	misidentified
OGLE005803.73-723602.0	ab	0.625510	SC8_FVI	$17.385 \pm 0.027$	$16.913 \pm 0.025$	blend
OGLE005806.86-723811.7	ab	0.614224	SC8_FVI	$18.561 \pm 0.033$	$18.261 \pm 0.044$	
OGLE005737.26-723819.1	ab	0.687028	SC8_FVI	$18.593 \pm 0.037$	$18.301 \pm 0.043$	
OGLE005752.74-723901.8	ab	0.557047	SC8_FVI	$18.883 \pm 0.043$	$18.606 \pm 0.053$	
2008-11-24						
OGLE004755.07-725141.5	ab	0.504549	SC4_FIV	$18.454 \pm 0.033$	$18.365 \pm 0.050$	
OGLE004805.17-725144.4	ab	0.509540	SC4_FIV	$19.002 \pm 0.058$	$18.626 \pm 0.058$	
OGLE004754.45-725212.1	ab	0.586127	SC4_FIV	$18.646 \pm 0.055$	$18.167 \pm 0.065$	
OGLE004756.26-725217.6	ab	0.592250	SC4_FIV	$18.700 \pm 0.039$	$18.446 \pm 0.045$	
OGLE004800.43-725222.7	ab	0.518919	SC4_FIV	$18.746 \pm 0.052$	$18.563 \pm 0.055$	
OGLE004758.51-725430.6	ab	0.618294	SC4_FIV	$18.803 \pm 0.040$	$18.535 \pm 0.055$	
OGLE004744.89-725530.1	c	0.297777	SC4_FIV	$19.035 \pm 0.056$	$18.798 \pm 0.067$	
OGLE004817.37-725536.5	ab	0.556467	SC4_FIV	$18.456 \pm 0.050$	$17.984 \pm 0.081$	
2008-12-14						
OGLE005451.72-723850.4	c	0.277966	SC7_FVII	$18.641 \pm 0.049$	$18.496 \pm 0.058$	contaminated
OGLE005527.97-724136.8	c	0.371404	SC7_FVII	$19.081 \pm 0.060$	$18.765 \pm 0.070$	
OGLE005621.27-730046.9	c	0.351118	SC7_FVIII	$18.833 \pm 0.044$	$18.654 \pm 0.103$	
OGLE005606.56-730242.1	ab	0.617223	SC7_FVIII	$18.469 \pm 0.032$	$18.167 \pm 0.039$	
OGLE005609.42-730323.2	ab	0.521781	SC7_FVIII	$18.976 \pm 0.049$	$18.614 \pm 0.055$	
2008-12-15						
OGLE010409.82-724611.9	ab	0.644261	SC10_FIX	$18.369 \pm 0.036$	$18.100 \pm 0.060$	
OGLE010442.62-724627.5	ab	0.614622	SC10_FIX	$18.582 \pm 0.045$	$18.282 \pm 0.048$	
OGLE010450.99-724700.3	ab	0.488994	SC10_FIX	$18.832 \pm 0.040$	$18.567 \pm 0.058$	
OGLE010501.92-724932.8	ab	0.496103	SC10_FIX	$19.258 \pm 0.061$	$18.742 \pm 0.060$	
OGLE010448.82-724945.3	ab	0.650334	SC10_FIX	$18.631 \pm 0.034$	$18.193 \pm 0.043$	
OGLE010432.13-724958.4	ab	0.629954	SC10_FIX	$18.513 \pm 0.035$	$18.413 \pm 0.113$	



Table 4. Averaged and extinction corrected magnitudes of observed RR Lyrae stars.

Star ID [OGLE]	Star type	Period [d]	Field name	$J_s$ [mag]	$K_s$ [mag]
OGLE004211.68-730329.2	ab	0.632047	SC2_FI	$18.663 \pm 0.033$	$18.344 \pm 0.062$
OGLE004225.29-730349.8	ab	0.699868	SC2_FI	$18.198 \pm 0.028$	$17.964 \pm 0.044$
OGLE004126.84-730355.2	ab	0.705041	SC2_FI	$18.485 \pm 0.038$	$18.208 \pm 0.057$
OGLE004154.36-730539.3	ab	0.524564	SC2_FI	$18.857 \pm 0.036$	$18.668 \pm 0.067$
OGLE004817.88-731815.2	ab	0.558981	SC4_FII	$18.356 \pm 0.039$	$18.091 \pm 0.046$
OGLE004744.69-731919.1	ab	0.598960	SC4_FII	$18.396 \pm 0.036$	$18.158 \pm 0.057$
OGLE004805.65-732033.9	ab	0.523798	SC4_FII	$18.735 \pm 0.031$	$18.549 \pm 0.067$
OGLE004724.96-731427.2	ab	0.614266	SC4_FIII	$18.586 \pm 0.058$	$18.385 \pm 0.040$
OGLE004649.00-731544.5	ab	0.665961	SC4_FIII	$18.285 \pm 0.031$	$18.013 \pm 0.045$
OGLE004650.36-731652.2	ab	0.630375	SC4_FIII	$18.378 \pm 0.026$	$18.206 \pm 0.048$
OGLE004755.07-725141.5	ab	0.504549	SC4_FIV	$18.340 \pm 0.031$	$18.299 \pm 0.035$
OGLE004805.17-725144.4	ab	0.509540	SC4_FIV	$18.780 \pm 0.046$	$18.536 \pm 0.044$
OGLE004754.45-725212.1	ab	0.586127	SC4_FIV	$18.476 \pm 0.051$	$18.133 \pm 0.056$
OGLE004756.26-725217.6	ab	0.592250	SC4_FIV	$18.616 \pm 0.034$	$18.381 \pm 0.034$
OGLE004800.43-725222.7	ab	0.518919	SC4_FIV	$18.756 \pm 0.040$	$18.524 \pm 0.044$
OGLE004758.51-725430.6	ab	0.618294	SC4_FIV	$18.624 \pm 0.035$	$18.393 \pm 0.039$
OGLE004744.89-725530.1	c	0.297777	SC4_FIV	$18.845 \pm 0.046$	$18.792 \pm 0.044$
OGLE004817.37-725536.5	ab	0.556467	SC4_FIV	$18.488 \pm 0.051$	$18.039 \pm 0.057$
OGLE005656.87-730850.2	ab	0.545403	SC7_FV	$18.652 \pm 0.063$	$18.310 \pm 0.046$
OGLE005616.96-730901.6	ab	0.615658	SC7_FV	$18.181 \pm 0.032$	$17.994 \pm 0.036$
OGLE005612.31-731222.5	ab	0.619898	SC7_FV	$18.656 \pm 0.028$	$18.481 \pm 0.039$
OGLE005806.86-723811.7	ab	0.614224	SC8_FVI	$18.471 \pm 0.033$	$18.224 \pm 0.044$
OGLE005737.26-723819.1	ab	0.687028	SC8_FVI	$18.503 \pm 0.037$	$18.264 \pm 0.043$
OGLE005752.74-723901.8	ab	0.557047	SC8_FVI	$18.793 \pm 0.043$	$18.569 \pm 0.053$
OGLE005527.97-724136.8	c	0.371404	SC7_FVII	$18.994 \pm 0.060$	$18.729 \pm 0.070$
OGLE005621.27-730046.9	c	0.351118	SC7_FVIII	$18.746 \pm 0.044$	$18.618 \pm 0.103$
OGLE005606.56-730242.1	ab	0.617223	SC7_FVIII	$18.382 \pm 0.032$	$18.131 \pm 0.039$
OGLE005609.42-730323.2	ab	0.521781	SC7_FVIII	$18.889 \pm 0.049$	$18.578 \pm 0.055$
OGLE010409.82-724611.9	ab	0.644261	SC10_FIX	$18.298 \pm 0.036$	$18.071 \pm 0.060$
OGLE010442.62-724627.5	ab	0.614622	SC10_FIX	$18.511 \pm 0.045$	$18.253 \pm 0.048$
OGLE010450.99-724700.3	ab	0.488994	SC10_FIX	$18.761 \pm 0.040$	$18.538 \pm 0.058$
OGLE010501.92-724932.8	ab	0.496103	SC10_FIX	$19.187 \pm 0.061$	$18.713 \pm 0.060$
OGLE010448.82-724945.3	ab	0.650334	SC10_FIX	$18.560 \pm 0.034$	$18.164 \pm 0.043$
OGLE010432.13-724958.4	ab	0.629954	SC10_FIX	$18.442 \pm 0.035$	$18.384 \pm 0.113$

Table 5. PL relations determined from averaged data of Table 4.

Calibration	$J$ slope	$J$ zero point	$K$ slope	$K$ zero point
Free fit	$-2.772 \pm 0.549$	$17.919 \pm 0.135$	$-3.104 \pm 0.494$	$17.598 \pm 0.122$
Sollima et al. (2008)	...	... $\pm$ ...	$-2.380$	$17.772 \pm 0.028$
Bono et al. (2003)	...	... $\pm$ ...	$-2.101$	$17.839 \pm 0.028$
Catelan et al. (2004)	$-1.773$	$18.159 \pm 0.031$	$-2.353$	$17.779 \pm 0.028$

Table 6. True SMC Distance Moduli determined from Different Calibrations.

Filter	Sollima et al. (2008)	Bono et al. (2003)	Catelan et al. (2004)
$J$	... $\pm$ ...	... $\pm$ ...	$18.946 \pm 0.181$
$K$	$18.965 \pm 0.161$	$19.002 \pm 0.165$	$18.966 \pm 0.161$